


ORIGINAL ARTICLE

Open Access



T1 ρ relaxation mapping in osteochondral lesions of the talus: a non-invasive biomarker for altered biomechanical properties of hyaline cartilage?

Balázs Bogner^{1,2*} , Markus Wenning^{3,4}, Pia M. Jungmann¹, Marco Reiser^{5,6}, Thomas Lange⁵, Marcel Tennstedt⁷, Lukas Klein⁷, Thierno D. Diallo¹, Fabian Bamberg¹, Hagen Schmal⁷ and Matthias Jung¹

Abstract

Background To evaluate T1 ρ relaxation mapping in patients with symptomatic talar osteochondral lesions (OLT) and healthy controls (HC) at rest, with axial loading and traction.

Methods Participants underwent 3-T ankle magnetic resonance imaging at rest and with 500 N loading and 120 N traction, without axial traction for a subcohort of 17/29 HC. We used a fast low-angle shot sequence with variable spin-lock intervals for monoexponential T1 ρ fitting. Cartilage was manually segmented to extract T1 ρ values.

Results We studied 29 OLT patients (age 31.7 ± 7.5 years, 15 females, body mass index [BMI] 25.0 ± 3.4 kg/m²) and 29 HC (age 25.2 ± 4.3 years, 17 females, BMI 22.5 ± 2.3 kg/m²). T1 ρ values of OLT (50.4 ± 3.4 ms) were higher than those of intact cartilage regions of OLT patients (47.2 ± 3.4 ms; $p = 0.003$) and matched HC cartilage (48.1 ± 3.3 ms; $p = 0.030$). Axial loading and traction induced significant T1 ρ changes in the intact cartilage regions of patients (loading, mean difference -1.1 ms; traction, mean difference 1.4 ms; $p = 0.030$ for both) and matched HC cartilage (-2.2 ms, $p = 0.003$; 2.3 ms, $p = 0.030$; respectively), but not in the OLT itself (-1.3 ms; $p = 0.150$; +1.9 ms; $p = 0.150$; respectively).

Conclusion Increased T1 ρ values may serve as a biomarker of cartilage degeneration in OLT. The absence of load- and traction-induced T1 ρ changes in OLT compared to intact cartilage suggests that T1 ρ may reflect altered biomechanical properties of hyaline cartilage.

Trial registration DRKS, DRKS00024010. Registered 11 January 2021, <https://drks.de/search/de/trial/DRKS00024010>.

Relevance statement T1 ρ mapping has the potential to evaluate compositional and biomechanical properties of the talar cartilage and may improve therapeutic decision-making in patients with osteochondral lesions.

Key Points

- T1 ρ values in osteochondral lesions increased compared to intact cartilage.
- Significant load- and traction-induced T1 ρ changes were observed in visually intact regions and in healthy controls but not in osteochondral lesions.
- T1 ρ may serve as an imaging biomarker for biomechanical properties of cartilage.

Keywords Ankle joint, Biomarkers, Hyaline cartilage, Magnetic resonance imaging, Talus

*Correspondence:

Balázs Bogner

balazs.bogner@uniklinik-freiburg.de

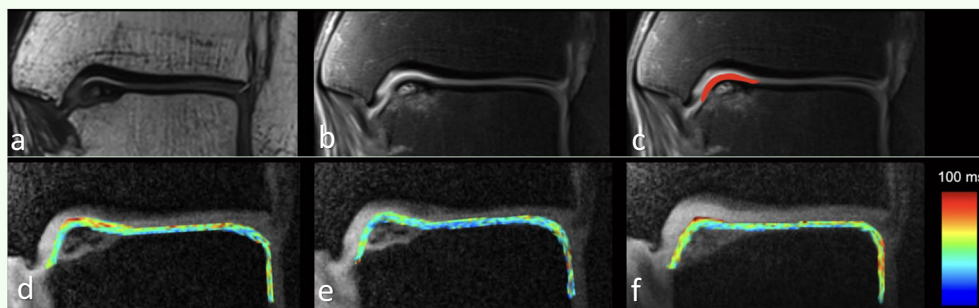
Full list of author information is available at the end of the article

Graphical Abstract

T1ρ relaxation mapping in osteochondral lesions of the talus: a non-invasive biomarker for altered biomechanical properties of hyaline cartilage?

 EUROPEAN SOCIETY OF RADIOLOGY

- T1ρ values in osteochondral lesions increased compared to intact cartilage.
- Significant load- and traction-induced T1ρ changes were observed in visually intact regions and in healthy controls but not in osteochondral lesions of the talus (OLT).
- T1ρ may serve as an imaging biomarker for biomechanical properties of cartilage.



(a) 3D SPACE and (b) proton density-weighted fat-saturated images from a patient with OLT at the medial talar shoulder, where bone marrow signal is altered, without apparent morphological changes. (c) The red overlay indicates the segmentation mask of the OLT cartilage. T1ρ maps (d) at rest, (e) with axial loading, or (f) traction. Note the decreased T1ρ induced by load and increased T1ρ induced by traction. High T1ρ = red; low T1ρ < 0 blue.

T1ρ mapping can evaluate composition and biomechanical properties of ankle cartilage. Early detection of changes may improve clinical decision making



**Eur Radiol Exp (2024) Bogner B, Wenning M, Jungmann PM, et al.
DOI: 10.1186/s41747-024-00488-4**

Background

Osteochondral lesions of the talus (OLT) refer to injuries involving talar articular cartilage and the subchondral bone [1]. OLTs frequently occur in physically active individuals and are reported in up to 73% of traumatic ankle injuries [2]. OLTs appear to be a significant joint-related risk factor for early osteoarthritis (OA) of the upper ankle joint, severely limiting athletic performance and potentially causing significant loss of quality of life in a young and athletic population [3, 4]. Timely therapeutical intervention to restore cartilage tissue may prevent the development of OA or delay its progression [5].

The underlying pathophysiology of OLTs is not fully understood. Repeated microtrauma to the articular cartilage as a possible causative factor may lead to disruption of the cartilage collagen network and secondary subchondral bone necrosis. Further, significant traumatic injury to the subchondral bone in the ankle may result in subsequent damage to the overlying articular talar cartilage. Regardless of the exact mechanism, chondral injuries are associated with a gradual decrease in cartilage proteoglycan content and an increase in water content due to disruption of the extracellular matrix [6, 7].

The detection of early changes in the cartilage tissue of OLT is a prerequisite for appropriate treatment [8].

Magnetic resonance imaging (MRI) enables noninvasive evaluation of the cartilage and subchondral bone and is, therefore, a valuable tool to assess OLT and related OA as a whole organ pathology [9]. However, conventional MRI techniques lack sensitivity in detecting subtle changes in the cartilage matrix which may be associated with early OA [10]. In contrast, quantitative MRI techniques, such as T2 relaxation time measurements and T1ρ relaxation time measurements provide information about compositional changes of the hyaline cartilage matrix in patients with OLT. T1ρ mapping allows for noninvasive quantitative assessment of biochemical changes of the cartilage matrix that are sensitive to early stages of OA which are not visible on morphological MRI [11, 12]. Since ultra-structural changes may correlate with the biomechanical performance of the hyaline cartilage, T1ρ mapping can be useful to noninvasively examine cartilage weight-bearing properties. Recent studies indicate that changes in T1ρ relaxation times may serve as an imaging biomarker of altered biomechanical properties of hyaline cartilage in patients with chronic ankle instability [13–15]. By applying *in situ* mechanical stress during the MRI examination the biomechanical and biochemical properties can be examined simultaneously [16–20]. Since chronic ankle instability can cause OLTs and eventually OA [21, 22], it

is of high clinical interest to assess potential biochemical and biomechanical changes derived from T1 ρ mapping in these patients.

The purpose of this study was to assess T1 ρ relaxation times in patients with OLT and healthy control subjects at rest, with axial loading and traction. We hypothesized that loading- and traction-induced changes in T1 ρ relaxation time may identify altered biomechanical properties of articular cartilage in patients with OLT.

Methods

The local Institutional Review Board approved the study which was prospectively registered at the German Clinical Trials Register (Trial registration: DRKS, DRKS00024010, January 11, 2021; <https://drks.de/search/de/trial/DRKS00024010>). Informed written consent was obtained from all individual participants included in the study. All procedures involving human participants were performed according to the ethical standards of the institutional and national research committee and to the Declaration of Helsinki in its current form.

Subjects

Inclusion criteria for healthy controls (HC) were the absence of symptoms at the ankle joint, stable ankles during clinical examination, no ankle sprain or any other traumatic ankle injury within the last two years, and a normal score according to the Cumberland Ankle Instability Tool-CAIT [23]. HC aged 18–50 years were randomly recruited from a community sample of students and employees working at the university. Patients with OLT were recruited from an outpatient clinic

specializing in the treatment of ankle injuries. There, the OLT diagnosis was based on clinical examination and confirmed by standard clinical MRI. After inclusion in this study, the OLT patients underwent a standardized morphological and quantitative MRI for this study (see below).

Inclusion criteria for patients were OLT-related symptoms such as load-induced pain or swelling for at least 6 months before enrollment. In addition, all patients had a history of ankle sprain not closer than 6 months before MRI examination. General exclusion criteria were age < 18 years, previous ankle surgery, traumatic ankle injury within the last 6 months, neurologic disorders, diabetes mellitus, and MRI contraindications. A subcohort of the HC group (17/29; 58.4%) included in this study was recruited from our previous study on T1 ρ mapping for chronic ankle instability (<https://pubmed.ncbi.nlm.nih.gov/35611813/>) [15]. This study focused on ankle instability and did not include any individuals with osteochondral lesions of the ankle joint and did not report on *in situ* axial traction. For this subcohort, no quantification of T1 ρ values under *in situ* axial traction was available. Therefore, only 12 HC were included in the statistical analysis involving the group and pairwise comparisons of T1 ρ changes after *in situ* traction. One patient was excluded from further analysis after initial MRI acquisition due to bilateral OLT (Fig. 1).

MRI acquisition

MRI of the ankle was performed using a 3-T scanner (Magnetom Trio, Siemens Healthineers, Erlangen,

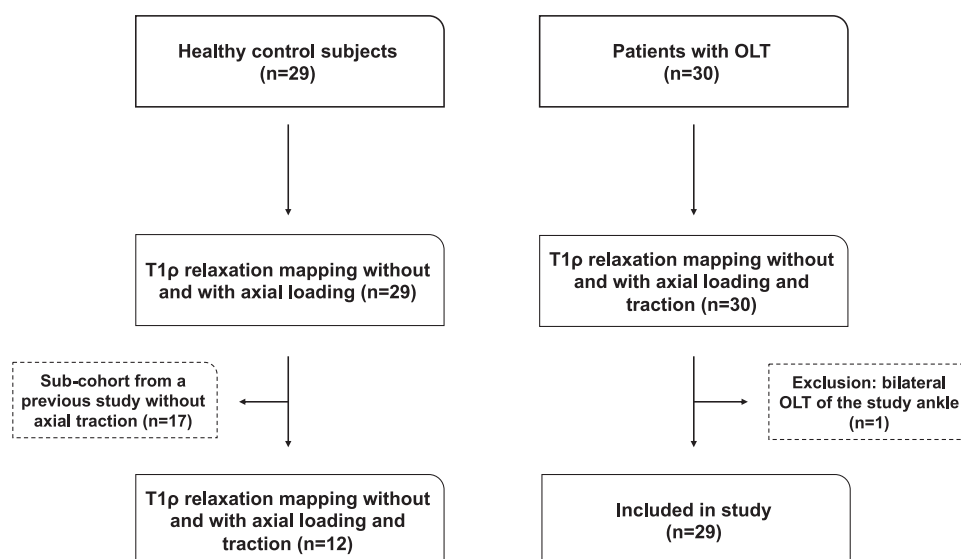


Fig. 1 Flow diagram of the study population. OLT, Osteochondral lesion of the talus

Germany), with a dedicated 8-channel multi-purpose coil (NORAS, MRI products, Höchberg, Germany) for signal reception. Patients with OLT and HC prospectively underwent MRI of the ankle at rest and with *in situ* axial loading of 500 N and traction of 120 N.

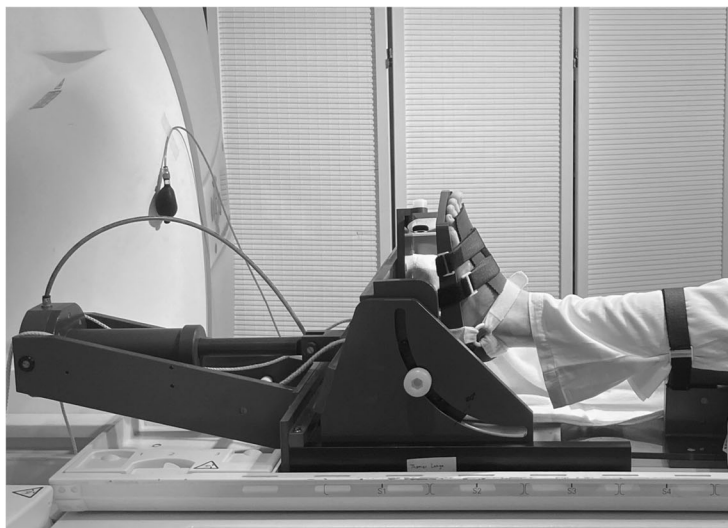
For morphological evaluation, we acquired:

- an isotropic three-dimensional proton density turbo spin echo sequence (Sampling Perfection with Application optimized Contrast using different flip angle Evolution—SPACE), with the following parameters: repetition time 900 ms; echo time 41 ms; flip angle 130°; voxel size $0.5 \times 0.5 \times 0.6 \text{ mm}^3$; phase encoding direction right-left; field of view $150 \times 150 \text{ mm}^2$; bandwidth 504 Hz/pixel; total acquisition time 4:55 min:s; and
- a coronal proton density turbo spin-echo with fat-suppression with the following parameters: repetition time 3.000 ms; echo time 32 ms; flip angle 160°; voxel size $0.4 \times 0.3 \times 3.0 \text{ mm}$; phase encoding direction anterior-posterior; field of view $150 \times 150 \text{ mm}^2$; bandwidth 248 Hz/pixel; total acquisition time 3:44 min:s.

For T1 ρ relaxation mapping we acquired a three-dimensional fast low-angle shot sequence with the following parameters: echo train duration 2.380 ms; repetition time 9.3 ms; echo time 4.62 ms; flip angle 10°; voxel size $0.3 \times 0.3 \times 2.4 \text{ mm}$; matrix size 256×256 ; in-plane resolution 0.3 mm; 12 partitions; readout direction right-left; phase

encoding direction anterior-posterior and feet-head; field of view $80 \times 80 \text{ mm}^2$; bandwidth 330 Hz/pixel; total acquisition time 5:00 min:s. For monoexponential pixel-by-pixel T1 ρ fitting, a spin-lock frequency of 500 Hz was used with five different spin-lock durations ($\tau = 0/10/20/30/40 \text{ ms}$). To avoid artifacts due to magnetic field inhomogeneities (ΔB_0), we implemented a ΔB_0 and B_1 insensitive spin-lock pulse cluster described by Witschey et al [24]. The preparation interval τ was divided into two periods with opposite spin-lock B_1 phase, separated by a 180° pulse for ΔB_0 refocusing ($90^\circ x - \tau/2 y - 180^\circ y - \tau/2 - y - 90^\circ x$). Fat saturation was applied between the spin-lock preparation interval and the fast low-angle shot module. The reproducibility of the T1 ρ mapping sequence used in this study was previously evaluated in a previous study. T1 ρ mapping was performed on two healthy volunteers, both at rest and under *in situ* axial loading of 200 N and 400 N, with a time interval of 6 months and 2 weeks between the measurements, respectively. T1 ρ mapping results showed high test-retest reproducibility between different time points and under different mechanical conditions [25].

All ankle MRI scans were performed (i) at rest, (ii) with *in situ* axial loading of 500 N, and (iii) with traction of 120 N with the examined ankle in a neutral position at 90° dorsiflexion. For both, *in situ* axial loading and traction, a custom-made arthrometer was used (Fig. 2). A minimum of 25 min of ankle rest was allowed before quantitative imaging due to the acquisition of morphological sequences and patient information. Before *in situ* axial loading, a



a



b

Fig. 2 Experimental setup for axial loading and traction of the ankle joint during acquisition. Mock-up experimental setup for axial (a) loading and (b) traction of the ankle joint. The custom-built arthrometer enables stable ankle positioning in a neutral position of 90° dorsiflexion. Note that the lower leg was fastened to a leg holder and a strap above the knee to prevent motion-induced artifacts. **a** Axial load was applied using a pneumatic loading system. **b** For axial traction, two 6-liter water-filled bags were connected to an ankle distractor foot strap through a cord pulley system

resting period of 15 min was obtained. Before axial traction, there was an additional resting period of 10 min during the setup of the traction arthrometer. For *in situ* axial loading, 500 N was applied using a pneumatic loading system to generate a significant loading effect without exciding the weight bearing on the ankle during single-leg stance. For axial traction, an ankle distractor foot strap was fixed around the talus using a cord and pulley system, connected to two 6-liter water-filled bags. During the MRI acquisition, subjects were fixed to the scanner bed with a pelvic belt. In addition, the lower leg was fastened to a leg holder and a strap above the knee to maintain the knee in full extension and to prevent motion-induced artifacts from mechanical loading and traction.

Image analysis

For morphological evaluation, all images were evaluated on a dedicated workstation (Dedalus Healthcare Group, Bonn, Germany). The location of the OLT was noted and classified as medial and lateral. To determine the size of the OLTs, maximum coronal and sagittal diameters were measured. The size of the OLT was calculated using the ellipse formula described by Choi et al [26]. Further, OLTs were graded according to Anderson et al by a board-certified radiologist with 10 years of experience in musculoskeletal radiology (T.D.D.) [27].

Quantitative MRI data was evaluated using a web-based medical image analysis platform (Nora Medical Imaging Platform, Freiburg; (available free of charge online: <https://www.nora-imaging.org/demo/index.php?viewer>). T1ρ maps were calculated by a mono-exponential pixel-by-pixel fit according to the following signal equation:

$$S(\tau) = S_0 \cdot \exp\left(-\frac{\tau}{T1\rho}\right)$$

where $S(\tau)$ is the measured signal intensity of the image for a given spin-lock duration τ and S_0 is the signal intensity for $\tau = 0$.

For T1ρ relaxometry, twelve coronal slices were reconstructed. To avoid partial volume artifacts due to the presence of potentially large amounts of synovial fluid at the peripheral regions of the cartilage layer, one anterior and one posterior slice were excluded from further analysis. Visually intact talar cartilage was manually segmented on the remaining ten coronal slices by two readers (B.B., 4 years of experience; M.T., 2 years of experience), carefully avoiding the corticalis, synovial fluid, and the OLT area. Subsequently, each volume of interest was divided into a medial and lateral subset at the midpoint of the superior articular surface of the talus according to the maximum curvature. The OLT cartilage

area was manually annotated in a separate volume of interest. To avoid bias due to regional differences in T1ρ values in the talar cartilage, we performed a regional matching to compare intact cartilage regions from OLT patients with cartilage from HC subjects [28]. T1ρ values obtained from talar cartilage regions contralateral to the OLT location were compared (Supplementary Fig. S1). Both readers were trained in cartilage segmentation by one of the senior authors (P.M.J., 15 years of experience). T1ρ data sets from ten independent subjects were analyzed by both readers (B.B., 4 years of experience; M.T., 2 years of experience) with at least 6 months between the two readings to assess interobserver agreement. In addition, to assess intraobserver agreement, measurements were repeated by one reader (B.B., 4 years of experience) after a minimum of four weeks to maintain retest independence.

For quality control, all segmentations were independently validated and adjusted where necessary by a board-certified radiologist (P.M.J., 15 years of experience).

Statistical analysis

Median T1ρ values were extracted from each volume of interest. Median T1ρ values of all volumes of interest showed normal distribution in quantile-quantile plots. Median T1ρ values of the OLT cartilage, visually intact cartilage regions of OLT patients, and matched cartilage of HC were compared using one-way analysis of variance (ANOVA) and post-hoc *t*-tests (Bonferroni-Holm corrected to avoid alpha error accumulation due to multiple testing). Changes in T1ρ relaxation times after axial loading and traction were compared using one-way ANOVA and post-hoc paired *t*-tests (Bonferroni-Holm). Due to unequal sample sizes, median T1ρ values of OLT cartilage obtained from different OLT grades were compared using the Kruskal-Wallis test and post-hoc Wilcoxon and paired Wilcoxon tests (Bonferroni-Holm corrected). To assess the intraobserver and interobserver agreement of image segmentation, we calculated the intraclass correlation coefficient (ICC, two-way mixed effect ANOVA). We used the following scale to interpret the ICC results: poor (ICC < 0.5), moderate (ICC 0.5–0.7), good (ICC 0.7–0.9), or excellent (ICC > 0.9) reproducibility [29]. The *p*-values lower than 0.05 were considered to be statistically significant. All statistical analyses were performed using R statistics (R-4.2.2 – R Core Team, <https://www.r-project.org/>).

Results

Patients characteristics

A total of 29 OLT patients (age 31.7 ± 7.5 years; body mass index (BMI) 25.0 ± 3.4 kg/m²; 15 females, 51.7%) and 29 HC (age 25.2 ± 4.3 years; BMI 22.5 ± 2.3 kg/m²; 17

females, 58.6%) were included in this study. Of the 29 OLT lesions, 24 (82.8%) were located on the medial talar shoulder. The OLT area was $108.8 \pm 57.5 \text{ mm}^2$ (mean \pm standard deviation). The majority of the OLTs (13/29, 44.8%) were graded as grade 3; the remaining were graded as grade 1 ($n = 3$; 10.3%), grade 2a ($n = 7$; 24.1%), grade 2b ($n = 4$; 13.8%), and grade 4 ($n = 2$; 6.9%). Patients' characteristics are described in Table 1.

Intraobserver and interobserver agreement

We found good to excellent intraobserver agreement for HC at rest (ICC 0.845), with *in situ* axial loading (ICC 0.990) and traction (ICC 0.947). For cartilage segmentation in the visually intact cartilage regions of OLT patients, the ICC was 0.973 at rest, 0.898 with axial loading, and 0.933 with traction. Furthermore, in the OLT

cartilage, ICC was 0.956 at rest, 0.986 with axial loading, and 0.901 with traction.

Also, the interobserver agreement was found to be good to excellent for cartilage segmentation in HC, at rest (ICC 0.807), under *in situ* axial loading (ICC 0.973), and under traction (ICC 0.788). Similarly, in the visually intact cartilage regions of OLT patients, interobserver agreement was good to excellent, at rest (ICC 0.929), with *in situ* axial loading (ICC 0.789), and with traction (ICC: 0.832). In the cartilage layer covering the OLT, the ICC was 0.909 at rest, 0.928 with *in situ* axial loading, and 0.864 with traction.

T1ρ values of OLT cartilage versus visually intact cartilage regions

At rest, we found significantly higher T1ρ values in the OLT cartilage ($50.4 \pm 3.4 \text{ ms}$) compared to visually intact cartilage regions of OLT patients ($47.2 \pm 3.4 \text{ ms}$; $p = 0.003$) and matched cartilage of HC ($48.1 \pm 3.3 \text{ ms}$; $p = 0.030$; Fig. 3). There was no significant difference in the OLT cartilage between different OLT grades ($p = 0.870$).

There was no significant difference between the visually intact cartilage regions of OLT patients and the matched cartilage of HC ($p = 0.280$). Furthermore, no significant regional differences in the talar cartilage were found in HC ($p = 0.077$). After axial loading, T1ρ values in the OLT cartilage ($49.2 \pm 4.33 \text{ ms}$) remained significantly higher than in the visually intact cartilage regions of OLT patients ($46.0 \pm 2.6 \text{ ms}$; $p = 0.008$), but not compared to the matched cartilage of HC (46.8 ± 3.8 ; $p = 0.090$). Similarly, after traction, OLT cartilage T1ρ values ($52.7 \pm 3.8 \text{ ms}$) were significantly

Table 1 Patient characteristics

	Healthy controls	OLT
Group size	29	29
Sex (males/females)	12/17	15/14
Age (years)	25.2 ± 4.3	31.7 ± 7.5
Body mass index (kg/m ²)	22.5 ± 2.3	25.0 ± 3.4
OLT location (medial/lateral)	—	24/5
OLT area (mm ²)	—	108.8 ± 57.5
OLT grade (1, 2a/b, 3, 4)	—	3/7/4/13/2
Cumberland Ankle Instability Tool	30	15.47 ± 6.73

Values are given as mean values \pm standard deviation
CAIT Cumberland ankle instability tool score, OLT Osteochondral lesion of the talus

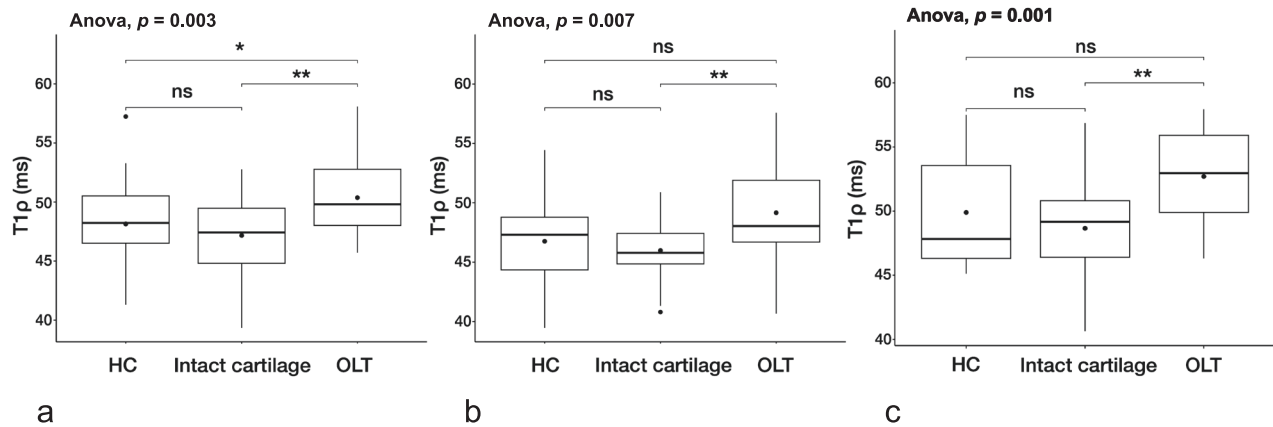


Fig. 3 T1ρ relaxation mapping in OLT cartilage versus visually intact cartilage regions. **a** T1ρ values in the OLT cartilage were significantly higher compared to visually intact cartilage regions. **b** After axial loading and **(c)** traction, T1ρ values in the OLT cartilage remained significantly higher than the intact cartilage regions in OLT patients, but not those of matched HC cartilage. There was no significant difference between visually intact cartilage regions in OLT patients and matched HC cartilage (**a–c**). Boxplots: the middle line represents the median; the upper and lower ends of the box represent the 75th and 25th percentiles, respectively. The black dot in the box represents the mean. * $p < 0.050$; ** $p < 0.010$; ns, Not significant. HC, Healthy controls; OLT, Osteochondral lesion of the talus

higher than those of visually intact cartilage regions of OLT patients (48.7 ± 3.9 ms; $p = 0.001$), but not compared to the matched cartilage of HC (49.9 ± 4.4 ; $p = 0.140$). During axial loading, T1 ρ values of grade 1 OLTs (39.14 ± 4.94 ms; $p = 0.042$) and grade 3 OLTs (48.24 ± 2.15 ms; $p = 0.042$), but not grade 4 OLTs (49.15 ± 4.09 ms; $p = 0.800$). There were no significant differences between grade 2, 3, and 4 OLTs (grade 2 *versus* 3; $p = 0.370$, grade 2 *versus* 4; $p = 0.727$, and grade 3 *versus* 4; $p = 0.606$). During axial traction, there were no significant differences in T1 ρ values between different OLT grades (grade 1 *versus* 2; $p = 0.769$, grade 1 *versus* 3; $p = 0.937$, and grade 1 *versus* 4; $p = 0.999$, grade 2 *versus* 3; $p = 0.387$, grade 2 *versus* 4; $p = 0.769$, and grade 3 *versus* 4; $p = 0.909$).

Both, after axial loading and traction, there was no significant difference between visually intact cartilage regions of OLT patients and matched cartilage of HC ($p = 0.420$ and $p = 0.410$, respectively).

Change in T1 ρ values after loading and traction

In situ axial loading led to a significant decrease in T1 ρ values in visually intact cartilage regions of OLT patients (mean difference -1.1 ms; $p = 0.030$) and in matched cartilage areas of HC (mean difference -2.2 ms, $p = 0.003$), but not in the OLT cartilage (mean difference -1.3 ms, $p = 0.150$; Fig. 4). Further, *in situ* axial traction resulted in a significant T1 ρ increase in visually intact cartilage regions of OLT patients (mean difference 1.4 ms, $p = 0.030$) and matched cartilage of HC (mean difference 2.3 ms, $p = 0.030$), but not in the OLT cartilage (mean difference 1.9 ms, $p = 0.150$; Figs. 4, 5). Axial loading did not induce significant changes in T1 ρ values in the OLT

cartilage in different OLT grades (grade 1, $p = 0.750$; grade 2, $p = 0.918$; grade 3, $p = 0.160$; and grade 4, $p = 0.999$). Similarly, there were no significant differences between OLT grades during axial traction (grade 1, $p = 0.750$; grade 2, $p = 0.453$; grade 3, $p = 0.129$; and grade 4, $p = 0.999$).

Discussion

In this cross-sectional study, we investigated T1 ρ relaxation times in the ankle joint at rest, with *in situ* axial loading and traction in patients with osteochondral lesions of the talus and healthy control subjects. At rest, we found significantly higher T1 ρ relaxation times in the OLT cartilage compared to visually intact cartilage regions within the same patients and matched cartilage of HC. However, there was no significant difference in T1 ρ values in the OLT cartilage between the different OLT grades. Following axial loading and traction, the OLT cartilage yielded consistently higher T1 ρ relaxation times compared to the visually intact cartilage regions of OLT patients. Axial loading led to a significant decrease in T1 ρ relaxation times in visually intact cartilage regions, but not in the OLT cartilage itself. Further, traction resulted in a significant increase in T1 ρ values in visually intact cartilage regions, but not in the OLT cartilage itself.

In early cartilage degeneration, an inverse correlation between T1 ρ relaxation times and relative proteoglycan concentration is well described in the current literature [11, 12, 30, 31]. In line with previous studies that assessed T1 ρ relaxation times in degenerated cartilage of the knee, this study found increased T1 ρ relaxation times in injured

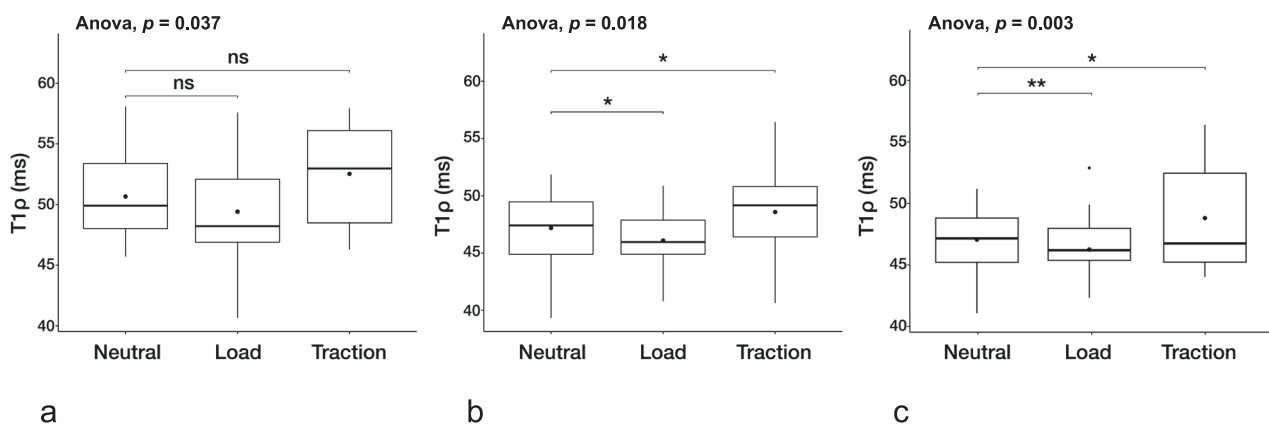


Fig. 4 Change in T1 ρ values after loading and traction. T1 ρ relaxation values at rest and with axial loading and traction (**a**) in the OLT cartilage, (**b**) in visually intact cartilage regions of OLT patients, and (**c**) in matched HC cartilage. **a** Both loading and traction did not induce significant T1 ρ changes in the OLT. Axial loading significantly decreased T1 ρ relaxation times in visually intact cartilage regions of (**b**) OLT patients and (**c**) matched HC cartilage, while traction led to a significant increase. Boxplots: middle line represents the median; the upper and lower ends of the box represent the 75th and 25th percentiles, respectively. The black dot in the box represents the mean. * $p < 0.050$; ** $p < 0.010$; ns, Not significant. HC, Healthy controls; OLT, Osteochondral lesion of the talus

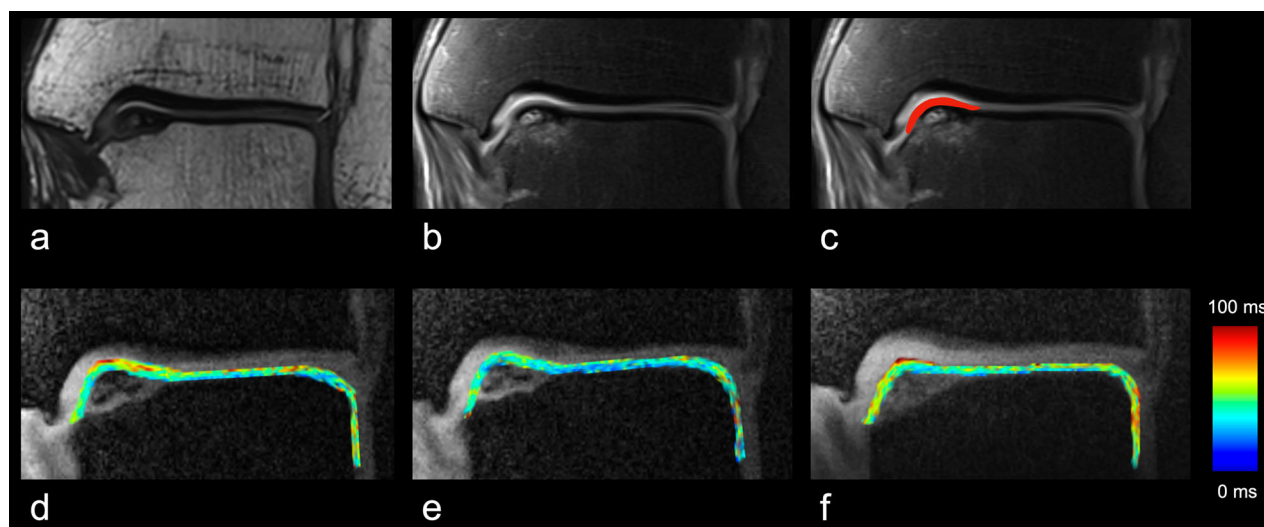


Fig. 5 Representative morphological images and T1 ρ maps under different mechanical conditions. Coronal (a) 3D SPACE (see text for details on the sequence) and (b) proton density-weighted fat-saturated images from a patient with OLT located at the medial talar shoulder. Note the altered bone marrow signal in the medial talar shoulder. There are no apparent morphological changes in the OLT cartilage. c The red overlay indicates the segmentation mask of the OLT cartilage, carefully avoiding the cortical bone and synovial fluid. Representative T1 ρ maps (d) at rest, (e) with axial loading, and (f) traction. Note the decreased T1 ρ values induced by 500 N axial load and increased T1 ρ values induced by 120 N traction. The blue color indicates low T1 ρ values and the red color indicates high T1 ρ values. HC, Healthy controls; OLT, Osteochondral lesion of the talus

cartilage regions in patients with OLT [32–34]. However, given the previously shown distinct biochemical, cellular, and biomechanical properties in healthy and damaged cartilage of the knee and ankle, a direct comparison of these results may be limited [35, 36]. In this study, the T1 ρ values of the OLT cartilage and matched HC cartilage showed significant overlap. Furthermore, no significant differences were observed in the OLT cartilage between different OLT grades. These findings indicate that T1 ρ relaxation mapping may serve as a complementary tool rather than providing robust stratification of cartilage damage in the OLT alone.

T1 ρ mapping may not only reflect cartilage composition but also its biomechanical properties. Changes in relaxation time in response to axial loading have been described as a surrogate for mechanical resilience with potential for *in vivo* monitoring of cartilage function [18–20, 37]. In this study, *in situ* axial loading induced a significant decrease in T1 ρ relaxation times in visually intact cartilage regions, but not in the OLT cartilage itself. These findings might reflect the relative increase in the proteoglycan concentration occurring due to reductions in tissue thickness and water content during axial loading [38]. Furthermore, load-induced changes in T1 ρ relaxation times might be accounted for by changes in collagen fiber orientation and hydration of hyaline cartilage [39]. In accordance, several studies reported decreased T1 ρ relaxation times in cartilage samples during acute loading [37, 40]. In contrast to the present findings, others

reported more pronounced changes in T1 ρ relaxation times in early degenerative than in intact cartilage [37, 39]. However, the knee and ankle joints have different responses to load profiles, *e.g.*, due to differences in the articular surface configuration and cartilage stiffness, which limits the comparability of the results across the knee and ankle joints [35]. Our results indicate important differences between healthy and damaged cartilage in the OLT. However, the load-induced changes in healthy cartilage regions and the OLT showed significant overlap. Based on these findings, T1 ρ relaxation mapping alone in response to axial loading may not provide a sufficient basis for differentiating early cartilage degeneration in the OLT cartilage.

In contrast to the widespread use of mechanical loading to quantitatively assess altered cartilage biomechanical properties, *in situ* axial traction in peripheral joint MR imaging has rather been used to improve diagnostic accuracy in morphological cartilage evaluation [41–44]. The present study investigated the impact of *in situ* axial traction on quantitative T1 ρ relaxation times and found a traction-induced increase in T1 ρ values in visually intact cartilage regions, but not in the cartilage covering the OLT. The underlying cartilage matrix changes remain unknown even though these findings may indicate that loading-unloading-induced nutrition of the cartilage is impaired. Moreover, axial traction may result in increased T1 ρ relaxation times due to increased cartilage water content and relative reduction in proteoglycan content [11].

Quantitative MRI studies investigating whole ankle cartilage degeneration in patients with OLT are scarce. Thus far, only one study has evaluated quantitative cartilage compositional properties before therapeutic intervention using T2 mapping [45]. Marik et al reported elevated T2 values in cartilage areas of OLT compared to morphologically intact adjacent cartilage and cartilage of healthy controls [45]. The T1ρ relaxation mapping performed in this study, assessed compositional and biomechanical cartilage properties in OLT, as T1ρ mapping has been reported to be more reproducible under *in situ* axial loading compared to T2 mapping [25]. Furthermore, T1ρ mapping has been described as a more sensitive method than T2 mapping for detecting early changes in OA due to its high sensitivity to cartilage proteoglycan content [46, 47]. In agreement with Marik et al [44], the current study found increased T1ρ relaxation times in the OLT cartilage compared to visually intact cartilage regions of the affected ankle and matched cartilage of HC.

Chronic ankle instability is linked to OLT [21, 22], which in turn may alter ankle biomechanics, cause chronic inflammatory symptoms, and worsen its instability if OLT becomes unstable [48, 49]. Furthermore, the progression of cartilage injury in OLT is associated with abnormal biomechanical characteristics of the damaged cartilage. The interaction between damaged cartilage and the surrounding healthy cartilage areas in the progression of OLT is not yet understood. Biomechanical performance and biochemical homeostasis seem to interact. Ruan et al reported altered mechanical stress distribution in the surrounding cartilage area of the OLT defect region using finite element analysis [50]. However, their analysis only focused on a small area of adjacent cartilage. In contrast to these findings, significant differences in T1ρ relaxation times between visually intact cartilage regions of OLT patients and matched cartilage of HC were not observed in the present study. Moreover, this finding was independent of axial loading or traction.

This study has several limitations. First, these results are limited by the relatively small sample size of patients with OLT, which is, however, comparable to most previous studies of this kind. Larger cohorts in multi-center settings of this rare disease should be designed to increase the robustness of these findings. Secondly, histopathological analysis of the cartilage was not performed and, as surgery was not always indicated, correlation with arthroscopic diagnosis of cartilage pathology was not possible. Therefore, it is challenging to determine the exact cartilage composition covering the OLT. Due to the subchondral bone involvement in the OLT, a natural tissue injury response may occur, ultimately leading to fibrocartilage formation [51, 52]. There are notable differences in T1ρ values comparing hyaline and fibrocartilage, which may

explain the different relaxation profiles in the OLT cartilage and intact cartilage regions of OLT patients and HC [53]. There are anatomic region-dependent differences in T1ρ relaxation times [28]. Due to the small sample size, pooled data from OLTs located both on the medial and lateral talar shoulder was included in the final analysis. This may have affected the overall error of the analysis. To achieve a more comprehensive assessment of the whole osteochondral unit, further studies should investigate the bone cartilage crosstalk. In addition, a separate analysis of deep and superficial cartilage layers was not performed. Several studies reported distinct response-to-loading patterns in the superficial and deep layers of the knee [20, 25, 54]. At the ankle joint, differentiation between cartilage layers is not feasible due to the small talar cartilage thickness and the limited spatial resolution of the MRI data. This study included relatively short rest periods before *in situ* axial loading. Different load-unload regimes are known to influence cartilage relaxation properties, which may account for the discrepancies when comparing our results to the current literature [55–57]. The repeatability of the T1ρ mapping sequence used in this study was evaluated in the knee cartilage of two healthy individuals. Compositional MRI of knee cartilage may not be directly comparable to that of the talus, particularly the OLT cartilage.

In conclusion, we showed that increased T1ρ relaxation times may serve as a sensitive imaging biomarker of early degenerative changes of hyaline cartilage in patients with OLT. Furthermore, the lack of load- and traction-induced T1ρ changes in OLT cartilage compared with visually intact cartilage regions may reflect altered biomechanical properties of damaged hyaline cartilage.

Abbreviations

ANOVA	Analysis of variance
BMI	Body mass index
HC	Healthy control
ICC	Intraclass correlation coefficient
MRI	Magnetic resonance imaging
OA	Osteoarthritis
OLT	Osteochondral lesion of the talus

Supplementary information

The online version contains supplementary material available at <https://doi.org/10.1186/s41747-024-00488-4>.

Additional file 1: Supplementary Fig. S1. Regional cartilage matching between OLT patients and healthy controls.

Acknowledgements

The authors particularly thank Dr. Ari Borthakur and Dr. Walter Witschey from the University of Pennsylvania for providing the T1ρ mapping sequence. BB is supported by the Berta-Ottenstein-Programme for Clinician Scientists, Faculty of Medicine, University of Freiburg. MJ and MW were supported by the Berta-Ottenstein-Programme for Clinician Scientists, Faculty of Medicine, University of Freiburg. The authors confirm that Large Language Models (LLMs) were not used in the preparation of this manuscript.

Authors contributions

BB conducted the analysis and interpretation of the experimental data related to T1ρ relaxation mapping in hyaline cartilage at the ankle joint and drafted the manuscript. MW and PMJ were involved in the study's conceptualization. MR and TL provided the data analysis tools. MT and LK collected data and performed manual cartilage segmentation. TDD conducted the morphological classification of the osteochondral lesions of the talus and carried out data analysis. MJ supported the data interpretation and was a major contributor to writing the manuscript. All authors critically reviewed and approved the final manuscript.

Funding

This study has received funding from the "Deutsche Arthrose-Hilfe e.V." (<https://www.arthrose.de/home>). Open Access funding enabled and organized by Projekt DEAL.

Data availability

The experimental dataset of the current study is not publicly available to preserve individuals' privacy under the European General Data Protection Regulation. A subset of the healthy controls (17/29) was previously reported in our study that assessed T1ρ relaxation mapping in individuals with chronic ankle instability. This dataset is available at the following URL: <https://pubmed.ncbi.nlm.nih.gov/35611813/>. This study focused on ankle instability and did not include any individuals with osteochondral lesions of the ankle joint and did not report on *in situ* axial traction.

Declarations

Ethics approval and consent to participate

Institutional Review Board (Ethik-Kommission Freiburg; 384/20) approval was obtained. Written informed consent was obtained from all subjects (patients) in this study. The authors disclose that "A subset of the healthy controls (17/29) was previously reported in our study that assessed T1ρ relaxation mapping in individuals with chronic ankle instability (REF). Our previous study focused on ankle instability and did not include any individuals with osteochondral lesions of the ankle joint and did not report on *in situ* axial traction".

Consent for publication

All patients declared consent for publication of the aggregated data.

Competing interests

The authors of this manuscript declare no relationships with any companies whose products or services may be related to the subject matter of the article.

Author details

¹Department of Diagnostic and Interventional Radiology, University Medical Center Freiburg, Faculty of Medicine, University of Freiburg, 79106 Freiburg, Germany. ²Berta-Ottenstein-Programme, Faculty of Medicine, University of Freiburg, Freiburg, Germany. ³Department of Orthopedics, BDH Klinik Waldkirch, 79283 Waldkirch, Germany. ⁴Praxis Drescher-Eberbach-Wenning, Orthopedic Surgeons, 79100 Freiburg, Germany. ⁵Division of Medical Physics, Department of Diagnostic and Interventional Radiology, University Medical Center Freiburg, Faculty of Medicine, University of Freiburg, 79106 Freiburg, Germany. ⁶Department of Stereotactic and Functional Neurosurgery, University Medical Center Freiburg, University of Freiburg, Faculty of Medicine, University of Freiburg, 79106 Freiburg, Germany. ⁷Department of Orthopedic and Trauma Surgery, University Medical Center Freiburg, University of Freiburg, Faculty of Medicine, University of Freiburg, 79106 Freiburg, Germany.

Received: 22 February 2024 Accepted: 16 June 2024

Published online: 24 July 2024

References

- McGahan PJ, Pinney SJ (2010) Current concept review: osteochondral lesions of the talus. *Foot Ankle Int* 31:90–101. <https://doi.org/10.3113/FAI.2010.0090>

- Posadzky M, Desimpel J, Vanhoenacker F (2017) Staging of osteochondral lesions of the talus: MRI and cone beam CT. *J Belg Soc Radiol* 101:1. <https://doi.org/10.5334/jbr-btr.1377>
- Huch K, Kuettner KE, Dieppe P (1997) Osteoarthritis in ankle and knee joints. *Semin Arthritis Rheum* 26:667–674. [https://doi.org/10.1016/s0049-0172\(97\)80002-9](https://doi.org/10.1016/s0049-0172(97)80002-9)
- Johnson VL, Giuffre BM, Hunter DJ (2012) Osteoarthritis: what does imaging tell us about its etiology? *Semin Musculoskelet Radiol* 16:410–418. <https://doi.org/10.1055/s-0032-1329894>
- Martin AR, Patel JM, Zlotnick HM et al (2019) Emerging therapies for cartilage regeneration in currently excluded 'red knee' populations. *NPJ Regen Med* 4:12. <https://doi.org/10.1038/s41536-019-0074-7>
- Rehmitz C, Klean B, Burkholder I et al (2017) Delayed gadolinium-enhanced MRI of cartilage (dGEMRIC) and T(2) mapping at 3T MRI of the wrist: feasibility and clinical application. *J Magn Reson Imaging* 45:381–389. <https://doi.org/10.1002/jmri.25371>
- Zengerink M, Szerb I, Hangody L et al (2006) Current concepts: treatment of osteochondral ankle defects. *Foot Ankle Clin* 11:331–359. <https://doi.org/10.1016/j.fcl.2006.03.008>
- Looze CA, Capo J, Ryan MK et al (2017) Evaluation and management of osteochondral lesions of the talus. *Cartilage* 8:19–30. <https://doi.org/10.1177/1947603516670708>
- Elias I, Jung JW, Raikin SM et al (2006) Osteochondral lesions of the talus: change in MRI findings over time in talar lesions without operative intervention and implications for staging systems. *Foot Ankle Int* 27:157–166. <https://doi.org/10.1177/107110070602700301>
- Choi JA, Gold GE (2011) MR imaging of articular cartilage physiology. *Magn Reson Imaging Clin N Am* 19:249–282. <https://doi.org/10.1016/j.mric.2011.02.010>
- Hatcher CC, Collins AT, Kim SY et al (2017) Relationship between T1rho magnetic resonance imaging, synovial fluid biomarkers, and the biochemical and biomechanical properties of cartilage. *J Biomech* 55:18–26. <https://doi.org/10.1016/j.jbiomech.2017.02.001>
- Regatte RR, Akella SV, Borthakur A et al (2002) Proteoglycan depletion-induced changes in transverse relaxation maps of cartilage: comparison of T2 and T1rho. *Acad Radiol* 9:1388–1394. [https://doi.org/10.1016/s1076-6332\(03\)80666-9](https://doi.org/10.1016/s1076-6332(03)80666-9)
- Wikstrom EA, Song K, Tennant JN et al (2019) T1rho MRI of the talar articular cartilage is increased in those with chronic ankle instability. *Osteoarthritis Cartilage* 27:646–649. <https://doi.org/10.1016/j.joca.2018.12.019>
- Song K, Pietrosimone B, Tennant JN et al (2021) Talar and subtalar T1rho relaxation times in limbs with and without chronic ankle instability. *Cartilage* 13:1402S–1410S. <https://doi.org/10.1177/1947603521994626>
- Lange T, Sturm L, Jungmann PM et al (2023) Biomechanical effects of chronic ankle instability on the talar cartilage matrix: the value of T1rho relaxation mapping without and with mechanical loading. *J Magn Reson Imaging* 57:611–619. <https://doi.org/10.1002/jmri.28267>
- Nieminen MT, Toyra J, Laasanen MS et al (2004) Prediction of biomechanical properties of articular cartilage with quantitative magnetic resonance imaging. *J Biomech* 37:321–328. [https://doi.org/10.1016/s0021-9290\(03\)00291-4](https://doi.org/10.1016/s0021-9290(03)00291-4)
- Subburaj K, Kumar D, Souza RB et al (2012) The acute effect of running on knee articular cartilage and meniscus magnetic resonance relaxation times in young healthy adults. *Am J Sports Med* 40:2134–2141. <https://doi.org/10.1177/0363546512449816>
- Nag D, Liney GP, Gillespie P et al (2004) Quantification of T(2) relaxation changes in articular cartilage with *in situ* mechanical loading of the knee. *J Magn Reson Imaging* 19:317–322. <https://doi.org/10.1002/jmri.20000>
- Nishii T, Kuroda K, Matsuoka Y et al (2008) Change in knee cartilage T2 in response to mechanical loading. *J Magn Reson Imaging* 28:175–180. <https://doi.org/10.1002/jmri.21418>
- Souza RB, Kumar D, Calixto N et al (2014) Response of knee cartilage T1rho and T2 relaxation times to *in vivo* mechanical loading in individuals with and without knee osteoarthritis. *Osteoarthritis Cartilage* 22:1367–1376. <https://doi.org/10.1016/j.joca.2014.04.017>
- Wang DY, Jiao C, Ao YF et al (2020) Risk factors for osteochondral lesions and osteophytes in chronic lateral ankle instability: a case series of 1169 patients. *Orthop J Sports Med* 8:2325967120922821. <https://doi.org/10.1177/2325967120922821>

22. Gianakos AL, Yasui Y, Hannon CP et al (2017) Current management of talar osteochondral lesions. *World J Orthop* 8:12–20. <https://doi.org/10.5312/wjo.v8.i1.12>
23. Hiller CE, Refshauge KM, Bundy AC et al (2006) The Cumberland ankle instability tool: a report of validity and reliability testing. *Arch Phys Med Rehabil* 87:1235–1241. <https://doi.org/10.1016/j.apmr.2006.05.022>
24. Witschey 2nd WR, Borthakur A, Elliott MA et al (2007) Artifacts in T1 rho-weighted imaging: compensation for B(1) and B(0) field imperfections. *J Magn Reson* 186:75–85. <https://doi.org/10.1016/j.jmr.2007.01.015>
25. Lange T, Knowles BR, Herbst M et al (2017) Comparative T(2) and T(1rho) mapping of patellofemoral cartilage under in situ mechanical loading with prospective motion correction. *J Magn Reson Imaging* 46:452–460. <https://doi.org/10.1002/jmri.25574>
26. Choi WJ, Park KK, Kim BS et al (2009) Osteochondral lesion of the talus: is there a critical defect size for poor outcome? *Am J Sports Med* 37:1974–1980. <https://doi.org/10.1177/0363546509335765>
27. Anderson IF, Crichton KJ, Grattan-Smith T et al (1989) Osteochondral fractures of the dome of the talus. *J Bone Joint Surg Am* 71:1143–1152
28. Horiuchi S, Yu HJ, Luk A et al (2020) T1rho and T2 mapping of ankle cartilage of female and male ballet dancers. *Acta Radiol* 61:1365–1376. <https://doi.org/10.1177/0284185120902381>
29. Koo TK, Li MY (2016) A guideline of selecting and reporting intraclass correlation coefficients for reliability research. *J Chiropr Med* 15:155–163. <https://doi.org/10.1016/j.jcm.2016.02.012>
30. Borthakur A, Wheaton A, Charagundla SR et al (2003) Three-dimensional T1rho-weighted MRI at 1.5 Tesla. *J Magn Reson Imaging* 17:730–736. <https://doi.org/10.1002/jmri.10296>
31. Collins AT, Hatcher CC, Kim SY et al (2019) Selective enzymatic digestion of proteoglycans and collagens alters cartilage T1rho and T2 relaxation times. *Ann Biomed Eng* 47:190–201. <https://doi.org/10.1007/s10439-018-02143-7>
32. Regatte RR, Akella SV, Wheaton AJ et al (2004) 3D-T1rho-relaxation mapping of articular cartilage: in vivo assessment of early degenerative changes in symptomatic osteoarthritic subjects. *Acad Radiol* 11:741–749. <https://doi.org/10.1016/j.acra.2004.03.051>
33. Li X, Benjamin Ma C, Link TM et al (2007) In vivo T(1rho) and T(2) mapping of articular cartilage in osteoarthritis of the knee using 3T MRI. *Osteoarthritis Cartilage* 15:789–797. <https://doi.org/10.1016/j.joca.2007.01.011>
34. Wyatt C, Guha A, Venkatchari A et al (2015) Improved differentiation between knees with cartilage lesions and controls using 7T relaxation time mapping. *J Orthop Translat* 3:197–204. <https://doi.org/10.1016/j.jot.2015.05.003>
35. Kraeutler MJ, Kaenkumchorn T, Pascual-Garrido C et al (2017) Peculiarities in ankle cartilage. *Cartilage* 8:12–18. <https://doi.org/10.1177/1947603516642572>
36. Juras V, Zbyn S, Mlynarik V et al (2016) The compositional difference between ankle and knee cartilage demonstrated by T2 mapping at 7 Tesla MR. *Eur J Radiol* 85:771–777. <https://doi.org/10.1016/j.ejrad.2016.01.021>
37. Souza RB, Stehling C, Wyman BT et al (2010) The effects of acute loading on T1rho and T2 relaxation times of tibiofemoral articular cartilage. *Osteoarthritis Cartilage* 18:1557–1563. <https://doi.org/10.1016/j.joca.2010.10.001>
38. Grunder W, Kanowski M, Wagner M et al (2000) Visualization of pressure distribution within loaded joint cartilage by application of angle-sensitive NMR microscopy. *Magn Reson Med* 43:884–891. [https://doi.org/10.1002/1522-2594\(200006\)43:6<884::aid-mrm15>3.0.co;2-u](https://doi.org/10.1002/1522-2594(200006)43:6<884::aid-mrm15>3.0.co;2-u)
39. Truhn D, Sondern B, Oehrl S et al (2019) Differentiation of human cartilage degeneration by functional MRI mapping—an ex vivo study. *Eur Radiol* 29:6671–6681. <https://doi.org/10.1007/s00330-019-06283-9>
40. Hamada H, Nishii T, Tamura S et al (2015) Comparison of load responsiveness of cartilage T1rho and T2 in porcine knee joints: an experimental loading MRI study. *Osteoarthritis Cartilage* 23:1776–1779. <https://doi.org/10.1016/j.joca.2015.05.019>
41. Llopis E, Cerezal L, Kassarian A et al (2008) Direct MR arthrography of the hip with leg traction: feasibility for assessing articular cartilage. *AJR Am J Roentgenol* 190:1124–1128. <https://doi.org/10.2214/AJR.07.2559>
42. Jungmann PM, Baum T, Schaeffeler C et al (2015) 3.0T MR imaging of the ankle: axial traction for morphological cartilage evaluation, quantitative T2 mapping and cartilage diffusion imaging—a preliminary study. *Eur J Radiol* 84:1546–1554. <https://doi.org/10.1016/j.ejrad.2015.04.023>
43. Baer TE, Stolley MP, Thedens DR et al (2006) Clinical tip: development of an ankle distraction device compatible with MRI and radiography. *Foot Ankle Int* 27:472–474. <https://doi.org/10.1177/107110070602700615>
44. Kohyama S, Tanaka T, Shimasaki K et al (2020) Effect of elbow MRI with axial traction on articular cartilage visibility—a feasibility study. *Skeletal Radiol* 49:1555–1566. <https://doi.org/10.1007/s00256-020-03455-3>
45. Marik W, Apprich S, Welsch GH et al (2012) Biochemical evaluation of articular cartilage in patients with osteochondrosis dissecans by means of quantitative T2- and T2-mapping at 3T MRI: a feasibility study. *Eur J Radiol* 81:923–927. <https://doi.org/10.1016/j.ejrad.2011.01.124>
46. Regatte RR, Akella SV, Lonner JH et al (2006) T1rho relaxation mapping in human osteoarthritis (OA) cartilage: comparison of T1rho with T2. *J Magn Reson Imaging* 23:547–553. <https://doi.org/10.1002/jmri.20536>
47. Sasho T, Katsuragi J, Yamaguchi S et al (2017) Associations of three-dimensional T1 rho MR mapping and three-dimensional T2 mapping with macroscopic and histologic grading as a biomarker for early articular degeneration of knee cartilage. *Clin Rheumatol* 36:2109–2119. <https://doi.org/10.1007/s10067-017-3645-2>
48. Li J, Wang Y, Wei Y et al (2022) The effect of talus osteochondral defects of different area size on ankle joint stability: a finite element analysis. *BMC Musculoskelet Disord* 23:500. <https://doi.org/10.1186/s12891-022-05450-2>
49. Hunt KJ, Lee AT, Lindsey DP et al (2012) Osteochondral lesions of the talus: effect of defect size and plantarflexion angle on ankle joint stresses. *Am J Sports Med* 40:895–901. <https://doi.org/10.1177/0363546511434404>
50. Ruan Y, Du Y, Jiang Z et al (2023) The biomechanical influence of defected cartilage on the progression of osteochondral lesions of the talus: a three-dimensional finite element analysis. *Orthop Surg* 15:1685–1693. <https://doi.org/10.1111/os.13753>
51. Jacob G, Shimomura K, Nakamura N (2020) Osteochondral injury, management and tissue engineering approaches. *Front Cell Dev Biol* 8:580868. <https://doi.org/10.3389/fcell.2020.580868>
52. Shapiro F, Koide S, Glimcher MJ (1993) Cell origin and differentiation in the repair of full-thickness defects of articular cartilage. *J Bone Joint Surg Am* 75:532–553. <https://doi.org/10.2106/00004623-199304000-00009>
53. Takayama Y, Hatakenaka M, Tsushima H et al (2013) T1rho is superior to T2 mapping for the evaluation of articular cartilage denaturalization with osteoarthritis: radiological-pathological correlation after total knee arthroplasty. *Eur J Radiol* 82:e192–e198. <https://doi.org/10.1016/j.ejrad.2012.11.031>
54. Subburaj K, Souza RB, Stehling C et al (2012) Association of MR relaxation and cartilage deformation in knee osteoarthritis. *J Orthop Res* 30:919–926. <https://doi.org/10.1002/jor.22031>
55. Schoenbauer E, Szomolanyi P, Shiomi T et al (2015) Cartilage evaluation with biochemical MR imaging using in vivo Knee compression at 3T-comparison of patients after cartilage repair with healthy volunteers. *J Biomech* 48:3349–3355. <https://doi.org/10.1016/j.jbiomech.2015.06.016>
56. Kessler DA, MacKay JW, McDonald S et al (2020) Effectively measuring exercise-related variations in T1rho and T2 relaxation times of healthy articular cartilage. *J Magn Reson Imaging* 52:1753–1764. <https://doi.org/10.1002/jmri.27278>
57. Cutcliffe HC, Davis KM, Spritzer CE et al (2020) The characteristic recovery time as a novel, noninvasive metric for assessing in vivo cartilage mechanical function. *Ann Biomed Eng* 48:2901–2910. <https://doi.org/10.1007/s10439-020-02558-1>

Publisher's Note

Springer Nature remains neutral with regard to jurisdictional claims in published maps and institutional affiliations.